Orai1 internalization and STIM1 clustering inhibition modulate SOCE inactivation during meiosis

Fang Yu[1], Lu Sun[1], and Khaled Machaca[2]

Department of Physiology and Biophysics, Weill Cornell Medical College in Qatar (WCMC-Q), Education City–Qatar Foundation, Doha, Qatar

Edited by David E. Clapham, Children's Hospital Boston, Boston, MA, and approved August 25, 2009 (received for review April 29, 2009)

Store-operated Ca^{2+} entry (SOCE) is a ubiquitous Ca^{2+} influx pathway activated in response to depletion of intracellular Ca^{2+} stores. SOCE is a primary modulator of intracellular Ca^{2+} dynamics, which specify cellular responses. Interestingly, SOCE inactivates during M phase but the mechanisms involved remain unclear. SOCE is mediated by clustering of the ER Ca^{2+} sensor STIM1 in response to Ca^{2+} store depletion, leading to gating of the plasma membrane SOCE channel Orai1. Here we show that SOCE inactivation in meiosis is the result of internalization of Orai1 into an intracellular vesicular compartment and to the inability of STIM1 to cluster in response to store depletion. At rest, Orai1 continuously recycles between the cell membrane and an endosomal compartment. We further show that STIM1–STIM1 interactions are inhibited during meiosis, which appears to mediate the inability of STIM1 to form puncta following store depletion. In contrast, STIM1–Orai1 interactions remain functional during meiosis. Combined, the removal of Orai1 from the cell membrane and STIM1 clustering inhibition effectively uncouple store depletion from SOCE activation in meiosis. Although STIM1 is phosphorylated during meiosis, phosphomimetic and alanine substitution mutations do not modulate STIM1 clustering, arguing that phosphorylation does not mediate STIM1 clustering inhibition during meiosis.

phosphorylation | store-operated calcium entry | trafficking

Depletion of intracellular (ER) Ca^{2+} stores results in the activation of Ca^{2+} influx from the extracellular space through SOCE (1). Recently the molecular determinants of SOCE have been elucidated (2). STIM1, an integral ER membrane protein with luminal EF hands, senses Ca^{2+} store depletion (3, 4), clusters in response to low ER Ca^{2+} and translocates to subplasma membrane domains (5, 6), where it gates the SOCE channel, Orai1 (7–10). Although physiologically SOCE is coupled to Ca^{2+} release from stores in response to G protein or tyrosine kinase coupled receptors, Ca^{2+} release per se is not required, rather it is coupling between luminal ER Ca^{2+} levels and Orai1 through STIM1 that regulates SOCE. The only known physiological case where this coupling is disrupted is during M phase of the cell cycle (11–13).

Fully grown oocytes in the vertebrate ovary are not fertilization competent and have to undergo a cellular differentiation pathway known as oocyte maturation to acquire the ability to activate at fertilization and transition into embryogenesis. A critical aspect of oocyte maturation is the differentiation of Ca^{2+} signaling pathways (14). Ca^{2+} is the universal signal for egg activation in all sexually reproducing species, and fertilization produces a spatially and temporally defined Ca^{2+} transient that is necessary and sufficient for egg activation (15). Remodeling of Ca^{2+} dynamics during *Xenopus* oocyte maturation affects multiple Ca^{2+} signaling pathways, primarily PMCA (16), the IP_3 receptor (17), and SOCE (12). SOCE is inhibited as the oocyte commits to meiosis (12), and MPF activation is sufficient for SOCE inactivation (12). As is the case in *Xenopus* eggs, SOCE inactivates during mitosis of mammalian cells (13, 18). Here we show that SOCE inactivation during meiosis is the result of Orai1 internalization and to the inability of STIM1 to cluster in response to store depletion.

Results and Discussion

Expression of mCherry–STIM1 and GFP–Orai1 in *Xenopus* oocytes shows that Orai1 traffics to the cell membrane, and STIM1 localizes to the ER as illustrated by its reticular distribution (Fig. 1*A*), and colocalization with GFP–KDEL (supporting information (*SI*) Fig. S1). Depletion of Ca^{2+} stores results in coclustering of STIM1 and Orai1 in the same focal plane in immature oocytes (Fig. 1*A*), which produces a large SOCE current (I_{SOC}) (Fig. 1*C*, Ooc). In contrast, in fully mature eggs arrested at metaphase of meiosis II, store depletion does not induce STIM1 or Orai1 clustering (Fig. 1*B*), and I_{SOC} does not develop (Fig. 1*C*, Egg). These data show that tagged human STIM1 and Orai1 are functional in *Xenopus* oocytes as they cluster in response to store depletion leading to the activation of I_{SOC}. Despite the overexpression of STIM1–Orai1, the oocyte cellular machinery remained effective at blocking I_{SOC} in M-phase, showing that these tagged proteins are useful reagents to investigate SOCE inactivation during meiosis, as they replicate the behavior of endogenous I_{SOC} (11).

Because Ca^{2+} release from stores mimics fertilization in fully mature eggs and results in egg activation, we resorted to the membrane permeant low affinity Ca^{2+} chelator TPEN to deplete Ca^{2+} stores without inducing a rise in cytosolic Ca^{2+} (19). Ca^{2+} store depletion using TPEN or other approaches, including IP_3 injection, ionomycin, or thapsigargin, produce similar coclustering of STIM1 and Orai1 (Fig. S2). Furthermore, expression of STIM1—but not Orai1—alone produced a small I_{SOC} compared to coexpression of both STIM1 and Orai1, arguing that STIM1 is limiting in *Xenopus* oocytes (Fig. 1*D*).

STIM1 distribution in eggs (Fig. 1*B*) reflects ER remodeling during meiosis as the ER forms large membrane patches during oocyte maturation as illustrated by GFP–KDEL expression (Fig. S1) (20). These patches are the result of complex ER membrane infoldings and have been described in details during maturation (20). STIM1 positive ER patches move closer to the cell membrane (Fig. 1*B*), reflecting the cortical enrichment of the ER during maturation (21). Orthogonal sections through z-stacks in oocytes show ER targeting of STIM1, and cell membrane localization of Orai1 (Fig. 1*A*). Note the microvilli structures in the oocyte orthogonal section (Fig. 1*A*). These microvilli are absent in eggs because of a dramatic decrease in cell membrane surface area during oocyte maturation (11, 21). This decrease is mediated by a block of exocytosis during maturation while endocytosis continues (22, 23). Store depletion in oocytes leads to coclustering of STIM1 and Orai1 in a single focal plane (Fig. 1*A*, Ortho). In contrast in eggs store depletion does not induce STIM1 clustering, rather STIM1 retains its distribution to ER patches and reticular structures (Fig. 1*B*). Accordingly, Orai1 distribution does not change and no Orai1 clusters are observed (Fig. 1*B*). However, we observed the appearance of an Orai1-positive intracellular vesicular compart-

Author contributions: F.Y. and K.M. designed research; F.Y., L.S., and K.M. performed research; F.Y., L.S., and K.M. analyzed data; and K.M. wrote the paper.

The authors declare no conflict of interest.

This article is a PNAS Direct Submission.

[1]F.Y. and L.S. contributed equally to this work.

[2]To whom correspondence should be addressed. E-mail: khm2002@qatar-med.cornell.edu.

This article contains supporting information online at www.pnas.org/cgi/content/full/0904651106/DCSupplemental.

CELL BIOLOGY

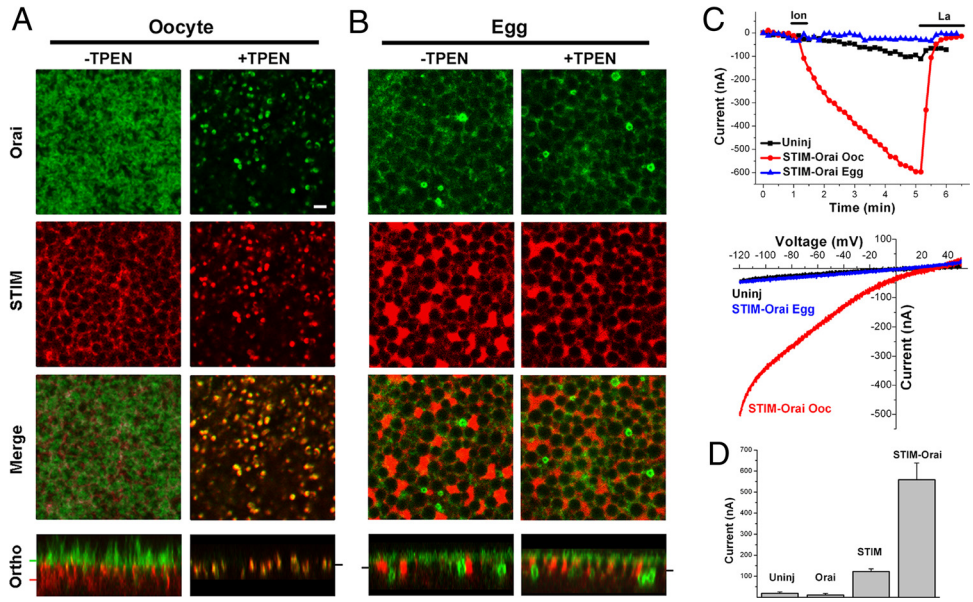

Fig. 1. STIM1–Orai1 subcellular distribution and interaction during meiosis. (*A* and *B*) STIM1–Orai1 clustering is inhibited in eggs. Oocyte were injected with mCherry–STIM1 and GFP–Orai1 and matured into eggs. Images show the distribution of Orai1 and STIM1 before and after store depletion with TPEN (5 mM). The plane at which the different sections are taken are indicated by the matching color bar in the orthogonal section. (Scale bar, 2 μm.) (*C*) Store depletion with ionomycin (10 μM) results in a large I_{SOC} in oocytes but not eggs. Time course and representative current-voltage relationships are shown. (*D*) I_{SOC} levels following injection of Orai1 and STIM1 alone or in combination (n = 5–23 cells; mean ± SE).

ment during meiosis (Fig. 1*B*). We refer to this intracellular enrichment of Orai1.

We then characterized the timing of STIM1 clustering inhibition and Orai1 internalization more carefully over the oocyte maturation time course. STIM1 maintains the ability to cluster in response to store depletion until 15–20 min after germinal vesicle (nuclear envelope) breakdown (GVBD). In oocytes, the majority of the GFP–Orai1 signal localizes to the cell membrane, however at high gain, GFP–Orai1 is also detectable in an intracellular vesicular compartment (Fig. 2*A*). This argues that Orai1 continuously recy-

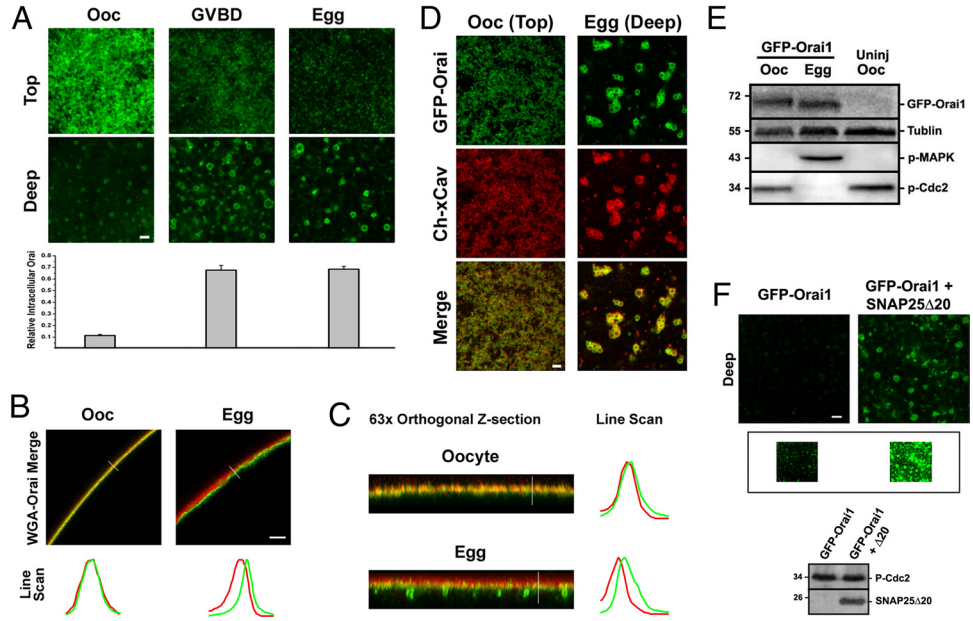

Fig. 2. Orai1 internalizes during meiosis. (*A*) Time course of Orai1 distribution during maturation. Images are from a z-section on each cell with the first image representing the top of the visible signal in the stack (Top) and the second image taken ≈2 μm deeper (Deep). Relative intracellular Orai1 represents the fluorescence intensity ratio of intracellular (Deep) versus surface (Top) Orai1 (n = 6; mean ± SE). (*B* and *C*) Orai1 injected oocytes and eggs costained with wheat germ agglutinin (WGA)-Alexa 633 to visualize the cell membrane at low (25×) (*B*) and high (63×) magnifications. (*C*) Line scans as indicated by the white line reflect the distribution of STIM1 and Orai1. Red, WGA; green, Orai1. (*D*) Confocal images from oocytes and eggs injected with GFP–Orai1 and mCherry-*Xenopus*-caveolin1 (Ch–xCav). (Scale bar, 2 μm.) (*E*) Westerns for GFP–Orai1, tubulin as the loading control, phospho-MAPK (P-MAPK), and phospho-Cdc2 (P-Cdc2). (*F*) Confocal images from GFP–Orai1 expressing oocytes injected with (*Right*) or without (*Left*) SNAP25Δ20 (30 ng) for 5 h. The inset shows the same images at high gain. Images were taken 3.5 μm into the cell. Western blots show SNAP25Δ20 expression and phosphorylation of MPF (inactive).

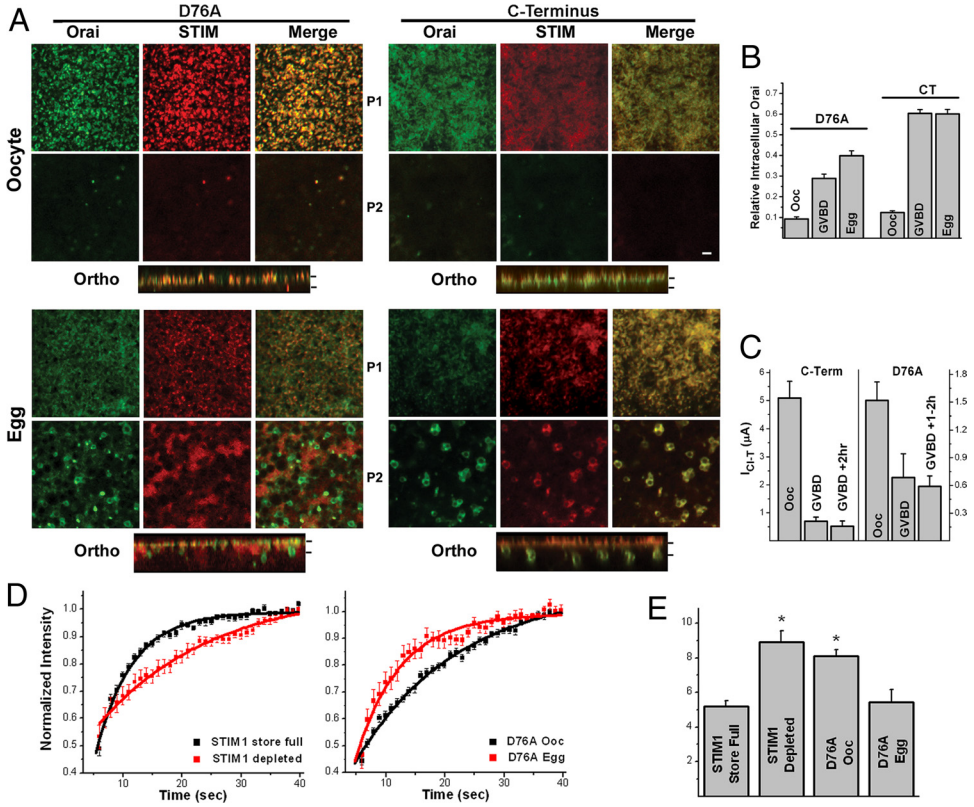

Fig. 3. Inactivation of SOCE mediated by constitutive active STIM1 mutants during meiosis. (*A*) The distribution of STIM1 and Orai1 following the expression of the constitutively active STIM1 mutants, $STIM1^{D76A}$ and the C terminus (CT-STIM1). Orthogonal views across the z-stack are also shown. Bars on orthogonal views indicate the planes at which the images where taken (P1, P2). (Scale bar, 2 μm.) (*B*) Estimates of total cell membrane GFP–Orai1 at different time points during oocyte maturation. GFP–Orai1 was estimated by quantifying membrane GFP fluorescence and multiplying it by the average cell capacitance at the equivalent time point. The data were normalized to the oocyte values ($n = 4$, mean ± SE). (*C*) SOCE levels during maturation were measured using the endogenous Ca^{2+}-activated Cl^- current ($I_{Cl\text{-}T}$) as a reporter. $I_{Cl\text{-}T}$ faithfully reports Ca^{2+} influx through SOCE channels (27, 28). (*D* and *E*) FRAP analysis of STIM1 and $STIM1^{D76A}$ diffusion. (*D*) Kinetics of the fluorescence recovery following photobleaching in cells expressing STIM1 before and after store depletion, and $STIM1^{D76A}$ in both oocytes and eggs (n = 12–26; mean ± SE). Data were fitted with a monoexponential decay function. (*E*) Recovery half-time ($T_{1/2}$) (n = 12–26; mean ± SE). The asterisk donates significantly different groups ($P \leq 0.00064$).

cles between the cell membrane and an endosomal compartment with a steady state enrichment at the membrane. The ratio of the intracellular versus surface signals shows gradual Orai1 internalization during maturation (Fig. 2*A*).

We then costained oocytes expressing GFP–Orai1 with wheat germ agglutinin to visualize the cell membrane (Fig. 2 *B* and *C*). Both low magnification cross-sectional images (Fig. 2*B*) and high magnification orthogonal views across z-stacks (Fig. 2*C*) show that Orai1 distribution shifts into a submembrane domain and primarily into an intracellular vesicular compartment (Fig. 2*C*, Egg).

To further characterize Orai1 trafficking during maturation, we generated an mCherry-tagged caveolin and tested its colocalization and trafficking with GFP–Orai1 (Fig. 2*D*), because there is some evidence in the literature that Orai1 may localize to lipid rafts (24, 25). Orai1 colocalizes and traffics with caveolin throughout oocyte maturation (Fig. 2*D*), arguing that Orai1 internalization occurs through caveolin-mediated endocytosis. The endosomal Orai1-positive vesicular compartment also contains caveolin and appears to be stable, arguing that Orai1 is not targeted for degradation. Indeed Western analysis of GFP–Orai1 reveals equivalent protein levels in oocytes and eggs showing that Orai1 is not degraded (Fig. 2*E*).

To directly test whether Orai1 continuously recycles between an endosomal compartment and the cell membrane in oocytes, we used a dominant negative SNAP-25 mutant (SNAP25Δ20) that blocks exocytosis in the oocyte (16). Because long-term SNAP25Δ20 expression relieves meiotic arrest, cells were injected with SNAP25Δ20 and tested 4–5 h later, a time point before the induction of maturation (16). Blocking exocytosis would be expected to shift the Orai1 steady-state distribution to the endosomal compartment, if Orai1 continuously cycles between the endosomal and cell membrane compartments. This is indeed the case as shown in Fig. 2*F*, where intracellular GFP–Orai1 is visible only at high gain in control oocytes (*Inset*).

To gain further insights into the regulation of Orai1 internalization and STIM1 clustering inhibition during maturation, we used 2 constitutively active STIM1 mutants, $STIM1^{D76A}$ and CT-STIM1. $STIM1^{D76A}$ is an EF-hand mutant that clusters and activates I_{SOC} independently of Ca^{2+} store content (3); and the C-terminal cytoplasmic domain of STIM1 (CT-STIM1) binds and activates Orai1 independently of cluster formation (26). In oocytes, $STIM1^{D76A}$ coclusters with Orai1, whereas CT-STIM1 colocalizes with Orai1 at the cell membrane, independently of cluster formation (Fig. 3*A*, Oocyte). Both mutants produce robust Ca^{2+} influx in oocytes (Fig. 3*C*, Ooc) with CT-STIM1 typically producing larger currents earlier, as it expressed significantly faster and to higher levels than $STIM1^{D76A}$. SOCE was measured in this case using the endogenous Ca^{2+}-activated Cl current $I_{Cl\text{-}T}$, which faithfully mirrors I_{SOC} (27, 28). Interestingly, SOCE mediated by both constitutively active mutants inactivates during maturation (Fig. 3*C*). Because the CT-STIM1 mutant activates SOCE without any cluster formation (Fig. 3*A*), it offers the opportunity to quantify the relative contribution of Orai1 internalization to SOCE inactivation independently of the modulation of STIM1 clustering. We hence estimated the

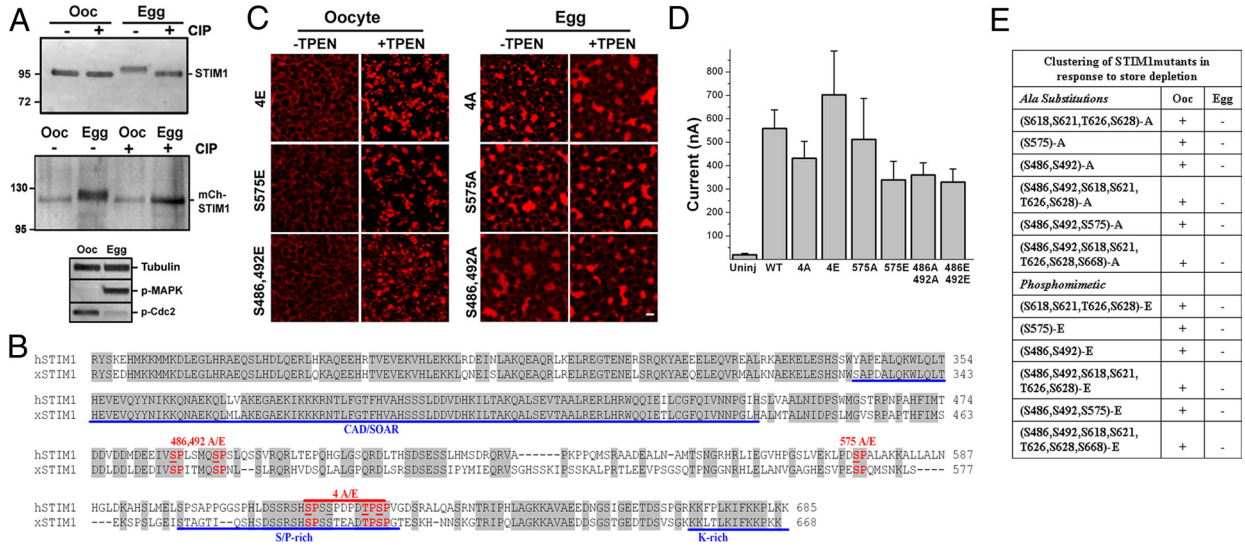

Fig. 4. Analysis of STIM1 phosphorylation during meiosis. (*A*) Both endogenous xSTIM1 and expressed hSTIM1 are phosphorylated during meiosis. Lysates from uninjected or mCherry–STIM1 injected oocytes and eggs were immunoprecipitated with anti-STIM1 antibody, left untreated (−) or treated with CIP (+), followed by Western blotting with either anti-STIM1 antibody to detect xSTIM1 or anti-DsRed antibody to detect mCherry–STIM1. (*B*) Sequence alignment of the C terminus of human (NP_003147) and *Xenopus* (AAI26012) STIM1. Conserved residues that match the S/T-P consensus for MAPK/MPF phosphorylation are indicated in red. Blue underlines indicate different STIM1 domains. (*C*) stim1 mutants behave in a similar fashion to WT-stim1. Example images of oocytes and eggs expressing STIM1^{4E}, STIM1^{S575E}, STIM1^{S486,S492E}, STIM1^{4A}, STIM1^{S575A}, and STIM1^{S486,S492A} mutants in the absence or presence of TPEN. (Scale bar, 2 μm.) (*D*) I_{soc} was measured as in Fig. 1*C* following coinjection with different STIM1 mutants with Orai1 (n = 4–23; mean ± SE). (*E*) Summary of the clustering ability in response to store depletion in all STIM1 mutants tested in both oocytes and eggs.

relative levels of total GFP–Orai1 at the cell membrane (Fig. 3*B*) and correlated them with the extent of current inhibition (Fig. 3*C*). There was a strong correlation between Orai1 internalization and current inhibition (Fig. S3). At the maximal levels of inhibition (>2 h after GVBD) current levels were inhibited by 90% and ≈82% of the cell membrane GFP–Orai1 was internalized. These estimates argue that Orai1 internalization is sufficient to inhibit 80–90% of SOCE activated by CT-STIM1 independently of STIM1 clustering.

When SOCE was activated by STIM1^{D76A} the estimated levels of total cell membrane GFP–Orai1 were similar to those observed for CT-STIM1 during maturation (Fig. 3*B*). This coincided with current inhibition although to a lesser extent than with the CT-STIM1 (Fig. 3*C*), leading to a poorer correlation between Orai1 internalization and current inhibition (Fig. S3). This is partly the result of the difficulty in recording currents in STIM1^{D76A} expressing cells past the 2 h after the GVBD time point as they lost cellular integrity. It could also reflect the increased potency with which preclustered STIM1^{D76A} activates SOCE as compared to CT-STIM1.

Interestingly, as STIM1^{D76A} was internalized during maturation clusters gradually disappeared and STIM1^{D76A} localized to ER membrane patches (Fig. 3*A*, D76A-Egg). STIM1^{d76a} that localizes to ER patches in eggs no longer interacts with internalized Orai1, which segregates to a distinct vesicular pool (Fig. 3*A*, D76A-Egg). In contrast, CT-STIM1 colocalizes with Orai1 in both oocytes at the cell membrane and in eggs as it cosegregates with Orai1 to intracellular vesicles (Fig. 3*A*, C terminus). This shows that STIM1–Orai1 interactions are functional in meiosis because CT-STIM1 can still associate with internalized Orai1 in eggs (Fig. 3*A*, C terminus Egg). However, STIM1^{D76A} and Orai1 do not colocalize in eggs. We postulate that this is because STIM1^{D76A}, unlike CT-STIM1, is anchored to the ER membrane and as the ER remodels in meiosis into large patches, STIM1^{D76A} is stripped away from Orai1, which trafficks to the endosomal compartment. Therefore, the lack of colocalization of STIM1^{D76A} and Orai1 is likely the result of their segregation to different compartments.

The fact that preformed STIM1^{D76A} puncta dissociate during maturation, argues that STIM1–STIM1 interactions are inhibited in meiosis, consistent with the inability of STIM1 to cluster in response to store depletion in eggs (Fig. 1*B*). This was confirmed by FRAP analyses of STIM1^{D76A} in both oocytes and eggs as compared to wild-type STIM1 before and after store depletion (Fig. 3 *D* and *E*). The mobile fraction was similar in all 4 cases (WT: 32.6 + 1.14, n = 24; WT ± TPEN: 30.05 ± 2.01, n = 14; STIM1^{D76A} Ooc: 35.67 ± 0.67, n = 26; STIM1^{D76A} egg: 31.43 ± 2.14, n = 12). As expected STIM1 diffusion was dramatically inhibited following store depletion (Fig. 3 *D* and *E*). The diffusion of preclustered STIM1^{D76A} in oocytes was similar to that observed in wild-type STIM1 after store depletion (Fig. 3 *D* and *E*). Interestingly, STIM1^{D76A} diffuses significantly faster in eggs, to a similar extent to the diffusion of STIM1 before store depletion in oocytes (Fig. 3 *D* and *E*). These data argue that STIM1–STIM1 interactions are disrupted in meiosis even in the preclustered STIM1^{D76A} mutant.

Collectively these data show that STIM1–Orai1 interactions are functional in meiosis, whereas STIM1–STIM1 interactions are disrupted. Furthermore, they show that in the case of the constitutively active CT-STIM1 mutant, Orai1 internalization is sufficient to largely inactivate SOCE in meiosis. Hence, SOCE inactivation during M phase is mediated by the inhibition of STIM1–STIM1 interaction leading to the inability of STIM1 to cluster in response to store depletion and to Orai1 internalization.

Given that MPF is sufficient to inactivate I_{SOC} (12), we tested whether STIM1 is phosphorylated during maturation. We show that both endogenous and expressed STIM1 are phosphorylated during meiosis, as indicated by the slower electrophoretic mobility in eggs as compared to oocytes (Fig. 4*A*), and the fact that treatment of the lysates with calf intestinal phosphatase reversed the slower mobility (Fig. 4*A*). Both the MAPK cascade and MPF, primary kinases that drive oocyte maturation (29), were activated in eggs but not oocytes (Fig. 4*A*). STIM1 contains several sites that match the minimal MAPK/MPF consensus (S/T-P) and are conserved between the human and *Xenopus* proteins (Fig. 4*B*, red). To map which sites are phosphorylated during maturation we performed mass spectrometry (MS) analyses on STIM1 immunoprecipitated (IP) from both oocytes and eggs (Fig. S4). MS detected 7 phosphorylated residues in eggs but no phosphorylation was detected in oocytes (Fig. S4*C*), confirming the biochemical analyses (Fig. 4*A*).

We performed the MS analyses 3 times on 2 different IPs, and detected only 1 site as consistently phosphorylated in eggs (Fig. S4). This suggests that although STIM1 is hyperphosphorylated in meiosis, this phosphorylation is quite heterogeneous. This argues against functionally significant site-specific phosphorylations, at least within the residues we detected as phosphorylated as we were unable to obtain complete sequence coverage over the entire protein. Nonetheless, to directly test whether phosphorylation at conserved MAPK/MPF sites is responsible for STIM1 clustering inhibition, we generated both phosphomimetic (S/T to E) and Ala substitution mutants (S/T to A) at conserved residues. If phosphorylation at these sites is sufficient to inhibit STIM1 clustering, then the phosphomimetic mutants should be unable to cluster in response to store depletion in oocytes, whereas Ala substitutions should reverse the clustering inhibition observed in eggs. We focused on the S/T-P sites that are conserved in both *Xenopus* and human STIM1 because both endogenous SOCE and SOCE mediated by human STIM1–Orai1 expression inactivate during maturation. We generated the mutants outlined in Fig. 4*E*, and in all cases tested the phosphomimetic mutations were unable to block STIM1 clustering in oocytes in response to store depletion, and the Ala substitution mutants were ineffective at reversing STIM1 clustering inhibition in eggs (Fig. 4 *C* and *E*). Examples of the mutants clustering behavior during oocyte maturation in response to store depletion are shown in Fig. 4*C*. In addition, the different mutants produced a typical I_{SOC} with an inward rectifying current–voltage relationship in oocytes (Fig. 4*D*). This argues that phosphorylation at these residues does not modulate STIM1 clustering (Fig. 4 *C*–*E*). The S618,S621,T626,S628E (Fig. 4*E*) mutant expressed in oocytes migrates with a slower electrophoretic mobility on SDS/PAGE in a similar fashion to phosphorylated STIM1 in eggs (Fig. S5). This argues that phosphomimetic mutations at these residues replicate STIM1 hyperphosphorylation observed in eggs. Since this mutant clusters normally in response to store depletion (Fig. 4 *C* and *E*), this suggests that hyperphosphorylation per se is not sufficient to block STIM1 clustering.

To address the relationship between the kinase cascade driving oocyte maturation and SOCE inactivation, we differentially manipulated MAPK and MPF independently and tested the effect on Orai1 and STIM1 (Fig. 5). Injection of MosRNA activates the entire cascade in a similar fashion to progesterone treatment (Fig. 5*A*), while preinjection of Wee inhibits MPF activation despite the high levels of MAPK activity produced by Mos injection. In contrast, injection of cyclin B RNA activates MPF initially followed by activation of the MAPK cascade because of a positive feedback loop between MPF and MAPK. Treating cells with U0126, a MEK inhibitor, before cyclin injection results in robust activation of MPF without MAPK activation. Confirmation that the treatments described above modulate the kinase cascade as expected is shown in Fig. 5*C*. We assessed Orai1 internalization and the ability of STIM1 to cluster in response to store depletion in the 4 treatment paradigms, leading to activation of either the MAPK cascade or MPF independently (Fig. 5). Although we did not carefully quantify Orai1 internalization, in all cases we observe an enrichment of Orai1 intracellularly (Fig. 5*B*), arguing that activation of either the MAPK cascade or MPF individually is sufficient to initiate Orai1 internalization. In contrast, as is the case in eggs matured with progesterone (Fig. 1*B*), STIM1 was unable to cluster when MPF was active (that is in the Mos, cyclin, and U-cylin treatments) independently of the activation state of MAPK (Fig. 5 *B* and *C*). When MPF was inhibited with Wee injection (Wee-Mos treatment), STIM1 clustered normally in response to store depletion (Fig. 5*B*, Wee-Mos). These data argue that MPF is required for STIM1 clustering inhibition; however, on the basis of the mutational analysis of MAPK/MPF consensus sites in STIM1 (Fig. 4), it is unlikely that MPF exhibits its effect by direct phosphorylation of STIM1.

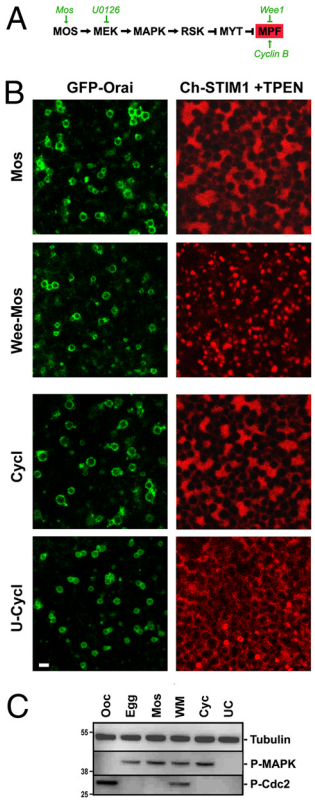

Fig. 5. Kinase-dependent inhibition of STIM1 clustering during meiosis. (*A*) Signaling cascade regulating *Xenopus* oocyte maturation. Oocytes expressing GFP–Orai1 and mCherry–STIM1 were untreated (Ooc) or treated with 5 μg/mL progesterone (egg); injected with Mos RNA (10 ng, Mos); injected with Wee1 RNA (10 ng) and incubated overnight before Mos RNA injection (Wee-Mos); injected with cyclin B1 RNA (10 ng, Cycl); or pretreated with U0126 (50 μM) for 1 h before cyclin B1 RNA injection (U-Cycl). Orai internalization is shown as a confocal section deep into the cell. STIM1 clustering is shown only after store depletion (+TPEN) (Scale bar, 2 μm.) The examples shown are representative of 6–8 cells for each treatment. (*C*) Lysates from cells analyzed in *B* tested for MAPK (P-MAPK) and Cdc2 (P-cdc2) phosphorylation.

Inactivation of Ca^{2+} influx during M phase of the cell cycle has been described during both mitosis of mammalian cells (13) and *Xenopus* oocyte meiosis (11), and hence appears to be a conserved mechanism during cell division. The exception is mammalian eggs, which undergo prolonged Ca^{2+} oscillations postfertilization and maintain an active SOCE (30). Elucidating the mechanisms controlling SOCE inactivation during meiosis will provide important insights into the regulation of Ca^{2+} signaling in preparation for fertilization and embryonic development. An inadequate Ca^{2+} signal at fertilization disrupts egg activation thus precluding development. Our results show that Orai1 continuously recycles at the cell membrane in oocytes, and that it is internalized during meiosis into a caveolin positive endosomal compartment.

Before the identification of STIM1 and Orai1 an exocytotic block in *Xenopus* oocytes was shown to effectively inhibits SOCE, which was interpreted to imply exocytosis-dependent insertion of SOCE channels following store depletion (31). Our data argue that the exocytosis block shifts the distribution of Orai1 to the intracellular pool hence contributing to SOCE inactivation. Oocyte maturation is associated with an almost 50% decrease in membrane surface area in preparation for embryonic divisions (11). However, the internalization of membrane proteins is selective as Ca^{2+}-activated Cl^- channels remain functional on the cell membrane in eggs, whereas other proteins such as the plasma-membrane Ca^{2+}-ATPase and β-integrin are internalized (14). The exocytosis block

CELL BIOLOGY

during maturation, while endocytosis continues, leads to enrichment of channels and transporters within intracellular vesicular compartments, which are eventually inserted into the basolateral membrane of newly forming blastomeres leading to the formation of the first polarized epithelium during embryogenesis (32). GFP–Orai1 distribution is not polarized in *Xenopus* oocytes as it is observed on both the animal and vegetal poles, consistent with the fact that Ca^{2+} influx occurs on both poles (28, 33).

Orai1 internalization is sufficient to largely inactivate I_{SOC} mediated by constitutively active STIM1 mutants, $STIM1^{D76A}$ and CT-STIM1, and the level of inactivation correlates with the extent of Orai1 internalization. Importantly analyses of STIM1 and Orai1 spatial distribution during meiosis following expression of the constitutive STIM1 mutants show that STIM1–Orai1 interactions are not affected during meiosis, showing that in meiosis if STIM1 is in the active conformation it is able to associate with Orai1. In contrast, STIM1–STIM1 interactions are abolished during meiosis as illustrated by the loss of $STIM1^{D76A}$ preformed puncta in eggs and STIM1 mobility in FRAP experiments. This explains the inability of STIM1 to form puncta in response to store depletion in eggs.

Furthermore, we show that MPF activation is necessary for inhibition of STIM1 clustering during maturation. However, despite the fact that STIM1 is hyperphosphorylated during maturation, the inhibition of STIM1 clustering does not appear to be the result of phosphorylation, because phosphomimetic and alanine substitution mutations at all conserved S/T-P sites were unable to modulate STIM1 clustering. These results argue that MPF does not block STIM1 clustering by direct phosphorylation of STIM1 in meiosis.

Materials and Methods

Molecular Biology and Electrophysiology. mCherry–STIM1 and GFP–Orai1 (7) were inserted into the *Xenopus* oocyte expression vector pSGEM (34), and C terminus and different STIM1 mutants were generated as described in *SI Text*. All point mutants were generated using the Quickchange mutagenesis kit and were verified by sequencing and by analytical endonuclease restriction enzyme digestion. RNA was transcribed using T7 RNA polymerase with T7 mMESSAGE mMACHINE kit (Ambion).

Xenopus laevis oocytes were prepared and handled as previously described (12). Measurements of the SOCE and Ca^{2+}-activated Cl^- currents were as previously described (11, 28), except that I_{SOC} was measured in 5Ca solution (in mM: 96 NaCl, 2.5 KCl, 5 $CaCl_2$, 10 Hepes pH7.4).

Imaging. Live cell imaging was taken by a Zeiss LSM710 confocal using a Plan Apo 63x/1.4 oil DIC II objective or a LD LCI Pln Apo 25X/0.8 oil objective. Images were analyzed using ZEN 2008 and MetaMorph and figures compiled using Adobe Photoshop.

Immunoprecipitation and Western Blotting. STIM1 was immunoprecipitated using an anti-STIM1 antibody (BD Transduction Laboratories). For dephosphorylation experiments, beads were incubated with calf intestinal phosphatase (New England BioLabs) for 1 h at 37 °C. Western blotting was performed using anti-DsRed (Clontech), anti-STIM1, or anti-SNAP25 (Stemberger Monoclonals) antibodies. Phospho-MAPK and phospho-Cdc2 Westerns were as previously described (35).

ACKNOWLEDGMENTS. We are grateful to Rich Lewis for the mCherry–STIM1 and GFP–Orai1 clones (7), to Rawad Hodeify for the initial characterization of these constructs in oocytes, to Mark Terasaki for the GFP–KDEL clone (20), to Shirley Haun for the phosphorylation of endogenous STIM1 Western and pSGEM-xCav construct, to Ricky Edmondson for help with MS methods, and to the Weill Cornell Medical College in Qatar (WCMC-Q) genomics core for sequencing various mutants. This work was funded by a grant from the National Institutes of Health GM061829, and startup funds from the Qatar Foundation and WCMC-Q.

1. Parekh AB, Putney JW (2005) Store-operated calcium channels. *Physiol Rev* 85:757–810.
2. Lewis RS (2007) The molecular choreography of a store-operated calcium channel. *Nature* 446:284–287.
3. Liou J, et al. (2005) STIM is a Ca2+ sensor essential for Ca2+-store-depletion-triggered Ca2+ influx. *Curr Biol* 15:1235–1241.
4. Roos J, et al. (2005) STIM1, an essential and conserved component of store-operated Ca2+ channel function. *J Cell Biol* 169:435–445.
5. Liou J, Fivaz M, Inoue T, Meyer T (2007) Live-cell imaging reveals sequential oligomerization and local plasma membrane targeting of stromal interaction molecule 1 after Ca2+ store depletion. *Proc Natl Acad Sci USA* 104:9301–9306.
6. Stathopulos PB, Li GY, Plevin MJ, Ames JB, Ikura M (2006) Stored Ca2+ depletion-induced oligomerization of stromal interaction molecule 1 (STIM1) via the EF-SAM region: An initiation mechanism for capacitive Ca2+ entry. *J Biol Chem* 281:35855–35862.
7. Luik RM, Wu MM, Buchanan J, Lewis RS (2006) The elementary unit of store-operated Ca2+ entry: Local activation of CRAC channels by STIM1 at ER-plasma membrane junctions. *J Cell Biol* 174:815–825.
8. Prakriya M, et al. (2006) Orai1 is an essential pore subunit of the CRAC channel. *Nature* 443:230–233.
9. Vig M, et al. (2006) CRACM1 is a plasma membrane protein essential for store-operated Ca2+ entry. *Science* 312:1220–1223.
10. Yeromin AV, et al. (2006) Molecular identification of the CRAC channel by altered ion selectivity in a mutant of Orai. *Nature* 443:226–229.
11. Machaca K, Haun S (2000) Store-operated calcium entry inactivates at the germinal vesicle breakdown stage of Xenopus meiosis. *J Biol Chem* 275:38710–38715.
12. Machaca K, Haun S (2002) Induction of maturation-promoting factor during *Xenopus* oocyte maturation uncouples Ca^{2+} store depletion from store-operated Ca^{2+} entry. *J Cell Biol* 156:75–85.
13. Preston SF, Sha'afi RI, Berlin RD (1991) Regulation of Ca^{2+} influx during mitosis: Ca^{2+} influx and depletion of intracellular Ca^{2+} stores are coupled in interphase but not mitosis. *Cell Regulation* 2:915–925.
14. Machaca K (2007) Ca^{2+} signaling differentiation during oocyte maturation. *J Cell Physiol* 213:331–340.
15. Stricker SA (1999) Comparative biology of calcium signaling during fertilization and egg activation in animals. *Dev Biol* 211:157–176.
16. El Jouni W, Haun S, Hodeify R, Hosein WA, Machaca K (2007) Vesicular traffic at the cell membrane regulates oocyte meiotic arrest. *Development* 134:3307–3315.
17. El Jouni W, Jang B, Haun S, Machaca K (2005) Calcium signaling differentiation during Xenopus oocyte maturation. *Dev Biol* 288:514–525.
18. Tani D, Monteilh-Zoller MK, Fleig A, Penner R (2007) Cell cycle-dependent regulation of store-operated I (CRAC) and Mg2+-nucleotide-regulated MagNuM (TRPM7) currents. *Cell Calcium* 41:249–260.
19. Hofer AM, Fasolato C, Pozzan T (1998) Capacitative Ca^{2+} entry is closely linked to the filling state of internal Ca^{2+} stores: A study using simultaneous measurements of I_{CRAC} and intraluminal [Ca^{2+}]. *J Cell Biol* 140:325–334.
20. Terasaki M, Runft LL, Hand AR (2001) Changes in organization of the endoplasmic reticulum during Xenopus oocyte maturation and activation. *Mol Biol Cell* 12:1103–1116.
21. Campanella C, Andreuccetti P, Taddei C, Talevi R (1984) The modifications of cortical endoplasmic reticulum during in vitro maturation of *Xenopus laevis* oocytes and its involvement in cortical granule exocytosis. *J Exp Zool* 229:283–293.
22. Colman A, Jones EA, Heasman J (1985) Meiotic maturation in Xenopus oocytes: A link between the cessation of protein secretion and the polarized disappearance of golgi apprati. *J Cell Biol* 101:313–318.
23. Leaf DS, Roberts SJ, Gerhart JC, Moore HP (1990) The secretory pathway is blocked between the *trans*-Golgi and the plasma membrane during meiotic maturation in Xenopus oocytes. *Dev Biol* 141:1–12.
24. Pani B, Singh BB (2009) Lipid rafts/caveolae as microdomains of calcium signaling. *Cell Calcium* 45:625–633.
25. Jardin I, Salido GM, Rosado JA (2008) Role of lipid rafts in the interaction between hTRPC1, Orai1, and STIM1. *Channels (Austin)* 2:401–403.
26. Huang GN, et al. (2006) STIM1 carboxyl-terminus activates native SOC, I(crac) and TRPC1 channels. *Nat Cell Biol* 8:1003–1010.
27. Hartzell HC (1996) Activation of different Cl currents in *Xenopus* oocytes by Ca liberated from stores and by capacitative Ca influx. *J Gen Phys* 108:157–175.
28. Machaca K, Hartzell HC (1999) Reversible Ca gradients between the sub-plasmalemma and cytosol differentially activate Ca-dependent Cl currents. *J Gen Phys* 113:249–266.
29. Nebreda AR, Ferby I (2000) Regulation of the meiotic cell cycle in oocytes. *Curr Opin Cell Biol* 12:666–675.
30. Igusa Y, Miyazaki S (1983) Effects of altered extracellular and intracellular calcium concentration on hyperpolarizing responses of the hamster egg. *J Physiol* 340:611–632.
31. Yao Y, Ferrer-Montiel AV, Montal M, Tsien RY (1999) Activation of store-operated Ca2+ current in *Xenopus* oocytes requires SNAP-25 but not a diffusible messenger. *Cell* 98:475–485.
32. Muller HA (2001) Of mice, frogs and flies: Generation of membrane asymmetries in early development. *Dev Growth Differ* 43:327–342.
33. Machaca K, Hartzell HC (1998) Asymmetrical distribution of Ca-activated Cl channels in *Xenopus* oocytes. *Biophys J* 74:1286–1295.
34. Villmann C, Bull L, Hollmann M (1997) Kainate binding proteins possess functional ion channel domains. *J Neurosci* 17:7634–7643.
35. Sun L, Machaca K (2004) Ca^{2+}cyt negatively regulates the initiation of oocyte maturation. *J Cell Biol* 165:63–75.